Available online at www.sciencedirect.com

ScienceDirect

Physics Procedia 56 (2014) 1024 – 1033

Physics Procedia

8th International Conference on Photonic Technologies LANE 2014

In-process evaluation of electrical properties of CIGS solar cells scribed with laser pulses of different pulse lengths

Klaus Zimmer[a,*], Xi Wang[a], Pierre Lorenz[a], Lukas Bayer[a], Martin Ehrhardt[a], Christian Scheit[b], Alexander Braun[b,]

[a]*Leibniz-Institut für Oberflächenmodifizierung e. V., Permoserstraße 15, 04318 Leipzig, Germany*
[b]*Solarion AG, Pereser Höhe 1, 04442 Zwenkau, Germany*

Abstract

The optimization of laser scribing for the interconnection of CIGS solar cells is a current focus of laser process development. In addition to the geometry of the laser scribes the impact of the laser patterning to the electrical properties of the solar cells has to be optimized with regards to the scribing process and the laser sources. In-process measurements provide an approach for reliable evaluation of the electrical characteristics. In particular, the parallel resistance R_p that was calculated from the measured I-V curves was measured in dependence on the scribing parameters of a short-pulsed ns laser in comparison to a standard ps laser at a wavelength of 1.06 µm. With low pulse overlap of ~ 20% a reduction of R_p to 2/3 of the initial value has been achieved for ns laser pulses. In comparison to ps laser slightly more defects were observed at the investigated parameter range.

Peer-review under responsibility of the Bayerisches Laserzentrum GmbH

Keywords: laser scribing; solar cell; CIGS; integrated interconnection; parallel resistance

1. Introduction

The scribing of thin films on different substrates attracts increasing attention in current applications for flexible electronics, roll-to-roll processing and large-area circuits. The fulfilment of the challenges for these applications by standard techniques of patterning like photolithography is critical and needs high efforts. Hence, laser scribing

* Corresponding author. Tel.: +49-341-2353287; fax: +49-341-2352584 .
E-mail address: klaus.zimmer@iom-leipzig.de

Peer-review under responsibility of the Bayerisches Laserzentrum GmbH
doi:10.1016/j.phpro.2014.08.014

presents particular advantages for thin-film patterning but needs optimization to fulfil at the same time small scribing size, high speeds, high scribing quality, and low costs in fabrication.

Thin-film solar cells (TFSC) attract a lot of attention due to saving material costs, decreasing of the device weight and competitive performance. $Cu(In,Ga)Se_2$ (CIGS) is one of the most promising semiconductor materials in thin-film photovoltaics because the theoretical photoelectrical conversion efficiency can be as high as 27% [1]. The evaluation of various aspects of solar cell fabrication made from different materials shows that CIGS is one of the most promising material systems for the future photovoltaic industry [2]. Recently an efficiency of 20.4% has been achieved on a flexible polymer substrate at laboratory conditions [3].

Nomenclature

A_{SC}	area of the solar cell
E_p	laser pulse energy
f	laser pulse repetition rate
G	conductance
G_P^{CC}	parallel conductance at circular scribing
l	length of the laser scribe
OV	laser pulse overlap
R_p	parallel resistance
t_p	laser pulse length
r	radius
v_s	laser spot scanning velocity
V	voltage
V_{OC}	open circuit voltage
σ^*_{SCA}	specific conductance of the solar cell area
σ^*_{LS}	specific conductance of the laser scribe
CIGS	copper-indium-gallium-(di)selenide
TCO	transparent conductive oxides
ps	picosecond

For solar module fabrication the solar cell material needs to be divided into many short-width cells that are interconnected in series to reduce the photocurrent and, in consequence, the resistance losses [4]. The usually applied interconnection method for solar cell modules is monolithic integrated interconnection (MII) [5]. An alternative approach is external integrated interconnection (EII) that supplies the advantage of complete deposition of every thin-film layer [6]. In the standard industry, the serial interconnection of cells is still based on mechanical scribing for the P2 and P3 processes [7, 8] but laser scribing holds a substantial potential for cost saving in production.

Selective removal of films for the P1, P2, and P3 process to the CIGS solar cell interconnections can be performed with different types of lasers [5, 7, 9, 10]. In dependence on the processes of laser – thin-film interaction different mechanisms of the thin-film removal are known that can be used for scribing single films or multi-layers. The most discussed process is direct laser ablation that describes an explosive evaporation process due to near-surface laser photon absorption (linear or non-linear) traditionally in a bulk sample. Within multilayer thin films the different material characteristics of the layers (e.g. optical absorption), film interference effects, and the irradiation set-up (front (film) via rear (glass) side laser irradiation) can determine the region of photon-matter interaction that can also be within the thin-film stack well below the surface. In this case a stress-assisted ablation or confined ablation mechanism is discussed wherein laser-induced mechanical processes assist the direct interaction of the laser photons. Such stress-related laser ablation processes are well known for scribing or material removal of amorphous silicon solar cells [11] but can also be achieved for CIGS-related solar cell materials [9]. Further, a solely mechanical driven delamination process of the CIGS/TCO thin-film stack from the molybdenum film of a complete CIGS solar cell has been demonstrated recently [12]. In this case mechanical shock waves induced by the UV laser

photon ablation of the polyimide substrate result in the delamination and the thin-film removal.

For film side scribing with particular laser-scribing conditions a delamination-like process can induce the scribing of CIGS solar cell layers [5, 13, 14]. Although the mechanism is not fully investigated yet, laser-induced thermal expansion or a confined subsurface evaporation drives an initial bulging of the film and then fractures it into tens of micrometre-sized flakes as it is seen in in situ shadowgraph images of Ref. [14]. In consequence of this approach a reduction of laser energy needed for scribing has been observed.

In this work we concentrated on the P3 scribing process of CIGS solar cells with ns laser pulses at a wavelength of 1.064 µm that is needed to isolate adjacent solar cell segments for realizing the integrated interconnection.

2. In-process measurements of electrical solar cell properties

The measurement of the influence of process parameter impacts on the properties of electronic devices is typically performed at the stage of a functional device. However, various effects from the different process steps of production are influencing the characterizing measurements. This is also the case for the photovoltaic (PV) industry where the I-V characteristics are finally measured to get information on the stability of the fabrication process parameters.

For characterizing the impact of laser processes in relation to the assessment of process parameters or laser devices regularly a sequential procedure of measuring the device properties, e. g. a solar cell, performing the laser processing and measuring the device again is utilized. However, different effects related to the measurements itself, the time shift between the measurements, the transport and the device aging are influencing the result and cannot be completely separated from the impact of the laser processing. In consequence, this sequential approach of laser process characterization is time consuming, needs high efforts and therefore requires statistical analyses.

2.1. In-process measurement approaches

In-process measurements are capable to reduce the impact of secondary effects and facilitate more stable and reliable measurements of the requested solar cell properties. The principle approach of the in-process approach for measuring the laser impact on the characteristics of solar cells is shown in Fig. 1.

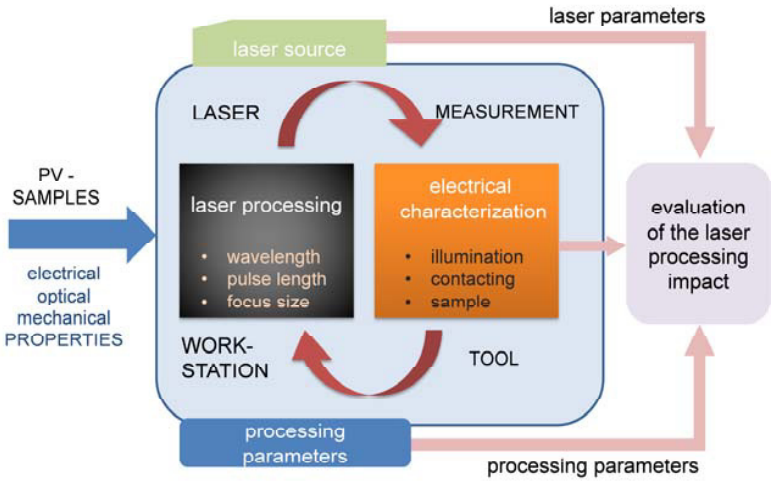

Fig. 1. Sketch of the in-process measurement approach for the characterization of the impact of laser irradiation on the properties of electronic devices, here shown for solar cells.

The properties of the laser scribe define the size of the dead area and the electrical losses which result from shunt formation due to defects and material modifications at the scribing area. Therefore, it is necessary to test the solar cell scribing conditions with a large number of different laser scribing parameters for optimization.

Different approaches to study the impact of the laser scribing on the solar cell properties are known [15, 16]. Typically a linear scribe can be applied to the solar cell, as depicted in Fig. 2 a) for example. Possible problems arise from the beginning and the end of the scribes due to acceleration of the laser spot. Further, at imperfect laser scribing parameters the solar cell is damaged severely and further measurements cannot be performed with this solar cell. However, the next solar cell needed for the studies has different properties and problems in evaluation of the electrical results can arise. The application of a scribing strategy based on nested patterns can help to solve the addressed problems.

2.2. Laser-scribing of layered systems to be studied with the approach

The current approach for the in-process measurements without contacting the laser-processed area was developed for the P3 scribe of thin-film solar cells [17]. However, the approach is suitable for systems sketched in Fig. 2 systems. The basic conditions to be fulfilled are that (i) the actual laser scribe should isolate the previous scribes from the electric circuit and (ii) the contact point to measure the electrical properties of the device defined by the current laser scribe should be not altered within a series of the in-process measurements. With this approach the following experimental problems in evaluation of the laser scribing impact on the characteristics of the scribe can be avoided:

- The electrical contacts are stable and have the same properties for all experiments.
- The electrical properties of the sample are almost equivalent for all experiments.
- The interaction strength of the laser with the sample is similar due to equivalent optical and thermal properties of the thin-film system to be scribed by the laser.

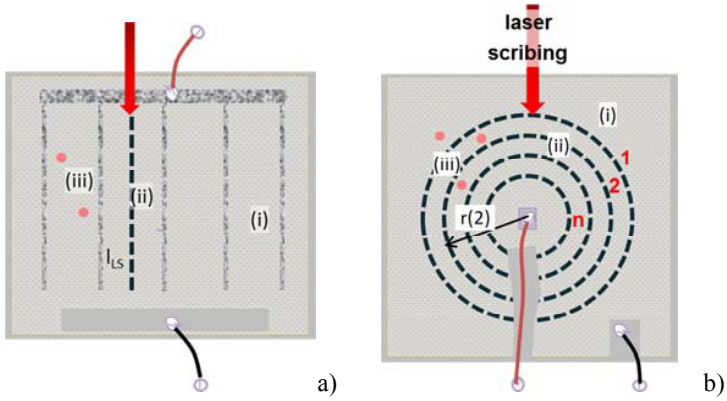

Fig. 2. Scribing technologies for electrical measurements of laser-induced shunt resistance measurements. (a) Linear scribes between the front contact fingers and (b) circular scribes at the same sample.

In addition to the primary goal of this approach to study the electrical effects of laser scribing also some properties of the layered system can be extracted from the investigations.

2.3. Considerations of the electrical model of laser-scribed solar cells

For laser-scribed layered systems the contributions of different sources of the sample to the external measured resistance for low-current conditions should be discussed. According to the equivalent circuit model of a solar cell such conditions can be achieved without a photo current (dark conditions) and without a substantial current flow through the diode ($V << V_{OC}$). At such conditions, the resistance of the thin films can be neglected so that the potentials in the conducting films are constant. The external measured current is the sum of the current across the solar cell material (i) and the contribution of the laser scribe (ii). The insulation material may feature an average specific conductivity and defects; both are specific for the sample. However, the influence of defects should not be discussed here.

Neglecting defects (shown as red dots in the figure) within the CIGS solar cell that are labelled with (iii) in Fig. 2 the parallel resistance of a solar cell scribed by the circular features can be calculated by

$$G_P^{CC} = \pi \cdot \left(\sigma_{SCA}^{*} \cdot r^2 + \cdot \sigma_{LS}^{*} \cdot r \right) \tag{1}$$

Each of the conductance components depends on the radius of the last laser scribe because the laser scribe isolates the enclosed area from the outside area that cannot longer contribute to the measured solar cell characteristics. Therefore, a quadratic function is found at sequential scribing of circular patterns. In addition, the long circumference of the circle allows a high sensitivity compared to a single line pattern.

For a single laser scribe between the contact fingers of a solar cell the parallel conductance is given by

$$G_P^{LC} = \left(\sigma_{SCA}^{*} \cdot A_{SC} + \cdot \sigma_{LS}^{*} \cdot l_{LS} \right) \tag{2}$$

σ_{SCA}^{*} is a coefficient representing the average electrical characteristic of the TFSC material.

3. Experimental

The experimental set-up is shown in Fig. 1 schematically and the utilized irradiation configurations are shown in Fig. 2. The linear scribe shown in Fig. 2 a is the standard approach but defects due to laser scribing, labeled as (ii), are influencing the electrical measurements of further laser scribes. The nested circular scribing approach that avoids such problems is shown in Fig. 2 b).

The two main parts of the whole experimental set-up comprise a laser workstation for performing the laser scribing of the thin film and the set-up for in-process measuring of the electrical properties. The samples were attached to the sample holder of the workstation and were connected by test needles (gold-coated industrial test needle, radius ≈ 0.4 mm, contact force approx. 0.5 N) for performing four-point measurements to record the I-V curves.

From the electrical measurements of the I-V curve the parallel resistance of the solar cell was calculated from the slope of the curve around zero voltage. The electrical measurements have been performed before and after the laser scribing to extract reliable results of the parallel resistance changes due to laser scribing.

Two different laser sources with an emission wavelength of 1.06 µm were used for laser scribing: a standard ps laser source with a pulse length of 12 ps and a ns laser with an adjustable pulse length (Pyrophotonics Lasers). The temporal pulse shape of the nanosecond pulse laser that was taken by photodiode with a rise time of 1 ns and a 2 GS (giga samples) storage oscilloscope is shown in Fig. 3. A unique characteristic of this source is the pulse length independent rise time of the laser pulse and the almost constant laser power within the pulse duration.

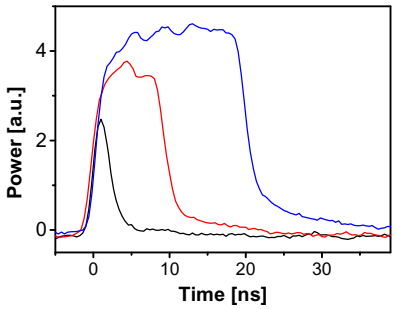

Fig. 3. Temporal shape of the ns laser pulses with different laser pulse lengths.

Both laser sources are installed into the laser workstation and applied for laser scribing of the CIGS solar cells. The laser beams were expanded to fit to the scanner aperture and were focused by the 163 mm scanner lens. The evaluation of the spot size by means of the D^2-method gives the spot size to be 13.7 µm and 12.4 µm for the ns and the ps laser, respectively.

4. Results and discussion

4.1. Morphology of P3 patterning – influence of the length of the ns laser pulse

For P3 scribing of CIGS solar cells different pulse lengths were applied to study the morphology of the scribe. The overlap was held low to get almost single pulse patterning and to achieve high scribing speed. Images of laser spots achieved with laser pulses of a length of 2 to 200 ns are shown in Fig. 4.

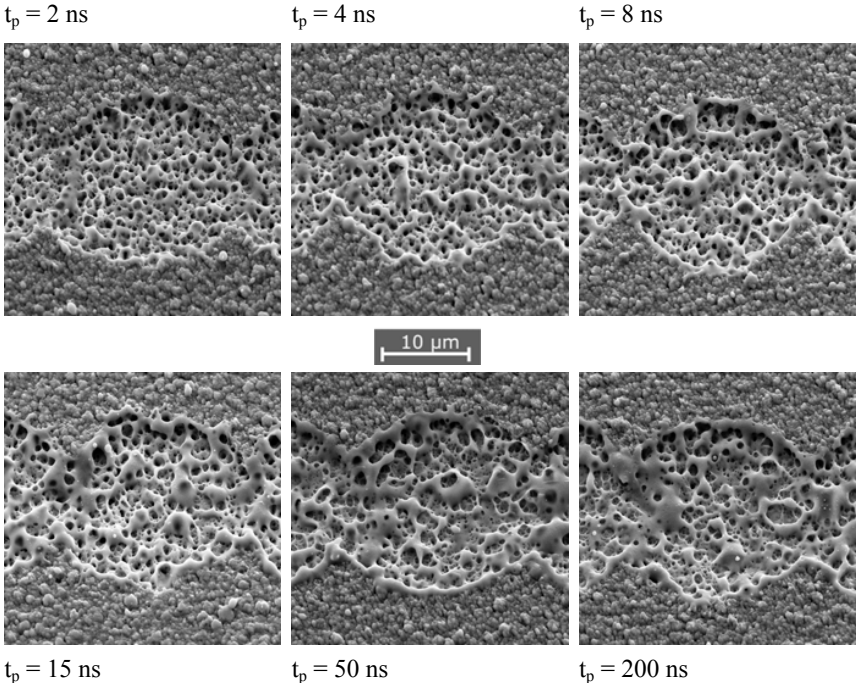

Fig. 4. (a) SEM images of P3 scribes with ns laser applying a pulse repetition rate of 60 kHz and a calculated overlap of approx. 20%. The pulse energy was in the range of 12 to 15 µJ.

The laser pulse energy was 12 µJ and 15 µJ for the longest ns pulses to get a similar overlap.

The TCO layer was removed with all laser pulse lengths; however, the surface morphology of the exposed CIGS is different. A clear trend to increased melting with rising laser pulse length is obviously. In addition a porous surface is characteristic of the exposed CIGS. The density of the pores is higher and the size of the pores is lower at shorter pulse duration. Both, the changed morphology of the pores and the larger melt pool areas can be explained with the pulse length. The longer the pulse duration the longer the melting lifetime of the CIGS can be expected. Therefore, small pores coalescence and form larger melted pools at higher pulse lengths. However, almost no alteration of the size of the removed TCO film from the CIGS can be observed although the pulse length increases substantially.

Considering the laser-induced temperatures that scales with $\sqrt{t_p}$ for bulk materials the longer laser pulses can heat up the material less than the shorter ones; however the size of the spots and their appearance is quite similar. Therefore a simple laser ablation mechanism is not probable for removing the TCO film. Taking into account the surface melt pool and the spot size a combined process of TCO delamination with melting of the CIGS below can be suggested. The delamination of the TCO can be driven by the melting evaporation of the CIGS below. Once the delamination starts the scattering of the laser radiation might be reduce the coupling into the TCO/CIGS interface and limits the melting although the laser pulse is not finished.

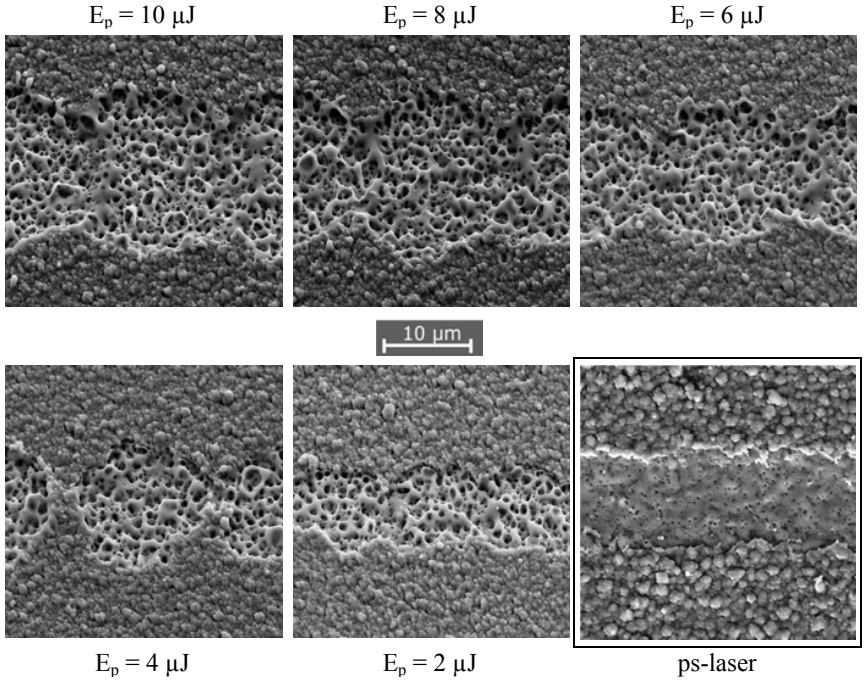

Fig. 5. SEM images of P3 scribes at a pulse length of 4 ns and a repetition rate of 60 kHz with different pulse energies. To keep the real overlap similar, the calculated pulse overlap increases from 36% to 65% with decreasing pulse energy. For comparison a ps-laser scribe (Ep = 1.1 µJ, f = 350 kHz, v_s = 1 m/s) is shown, too.

From the functional point of view the P3 scribe is an insulation scribe; the TCO film is clearly removed within the scribe although the pulse overlap is low. However, shunt formation due to laser scribing has to be avoided as well. Shunts connect the TCO film with the Mo back contact; into the solar cell a pn junction is formed that determines the current to the Mo film. Due to laser scribing molten CIGS may be transformed into a conductive phase that can form shunts to the TCO. Therefore, this molten material has to be in contact with the TCO film.

Because the lowest melting has been observed for short ns pulse lengths the influence of the pulse energy was studied for these parameters. The SEM images in Fig. 5 show the dependence on the applied pulse energy. With

reduced pulse energy the line width decrease as expected due to the Gaussian spot profile. The porous bottoms of the spot are nearly unaffected by the pulse energy, however, at the lowest energies less splashes at the TCO-film edge can be supposed.

For comparison the image of a ps laser spot is added to Fig. 5. The typical ripples for multi-pulse (3) ultrashort pulse ablation can be seen. Here a clear nearly melt-free border of the TCO can be seen. In the center slight signs of melting are visible.

The SEM images of figures 4 and 5 suggest that the ns laser patterning of the TCO film from CIGS solar cells is a single-pulse, laser-induced stress-related process. At the lowest pulse energy studied (2 µJ) also single pulse TCO ablation (at higher scanning speeds, not shown here) has been observed. No melting of the grainy TCO film that indicates melting can be observed. However, the longer the ns laser pulses the more melting can be seen at the bottom of the grooves. This shows clearly that not the TCO but the CIGS below the TCO absorbs sufficient laser energy. Further, the volumetric energy density for TCO removal was determined from the experimental results near the ablation threshold and from thermodynamic data considering sublimation of the TCO to be 12 J/cm³ and 25 J/cm³, respectively. The comparison of the experimental value with the proposed 100 J/cm³ required for direct ablation (see Ref. [18]) and the energy for sublimation neglecting TCO heating suggest a stress-assisted, CIGS interface located laser ablation mechanism. The ps laser the needed energy density is well below 10 J/cm³. Further, according to Ref. [19] the threshold fluence of TCO ablation with 1.064 µm ns laser is approximately 3 J/cm² and much higher to the here observed experimental value.

The white light interference microscopic image of a ns laser scribed CIGS sample (see Fig. 6) clearly shows the almost homogeneous removal of the TCO layer with one pulse and the melting of the CIGS film below the TCO within the TCO ablation process.

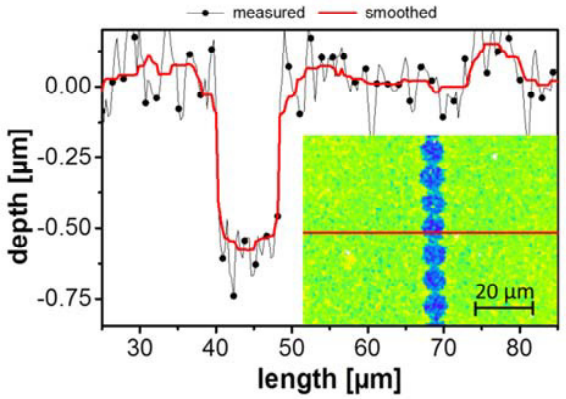

Fig. 6. Depth profile and white light interference microscopy image of ns laser scribed CIGS solar cell material. The steep edges and the uniform depth across the laser spot is seen that point to a delamination process. The roughness at the bottom is due to the melting of the CIGS (t_p = 2 ns; f = 60 kHz; E_p = 12 µJ; v_s= 1.3 m/s).

The steep edges of the removed TCO film and the flat bottom of the grooves that are made by a single laser pulse (the pulse overlap is ≈ 20%) is also a clear indication for the stress-assisted CIGS interface-located ablation mechanism of the TCO layer.

4.2. Electrical characterization of P3 scribes for ns laser

First standard CIGS solar cells were scribed with the ns laser between the front contact fingers (see Fig. 2 a) for evaluation of the laser scribing impact to the parallel resistance. With each scribe of 20 mm length the parallel resistance of the scribed CIGS solar cell drops and reduces the sensitivity of the next measurements for detectable laser-induced defects. Hence, the CIGS sample must be exchanged regularly. With each solar cell sample their properties are also different as seen in Table 1. As seen the initial parallel resistance varies strong due to defects or

quality differences and a clear trend of the influence of laser processing parameters is hardly to extract from the measurements.

Table 1. Parallel resistance R_p and change of the parallel resistance ΔR_p of CIGS solar cells after linear scribing at a real pulse overlap of approx. 20% with different laser parameters.
* These results are due to a defect from the mechanical scribing before laser scribing.

E_p [µJ]	t_p [ns]	R_p [Ω]	ΔR_p [Ω]
10	1	723.36	-113.87
15	1	565.5	-52.26
5	1	337.97	-23.34
10	5	167.07	-41.89
20	5	340.78	-176.74
12	5	122.42	-3.45
10	10	82.846	3.52*
12	10	741.89	-439.21

Therefore the parallel resistance has been measured by an in-process approach that allows the electrical characterization of the samples in the laser workstation. The developed in-process measurement tool was utilized for this purpose. The nested circular scribe methodology (see Fig. 2 b) is described in Ref. [17]. A series of parallel resistance measurements of one sample to study various laser scribing parameters for P3 scribing are shown in Fig. 7. Before the experiments the CIGS cell material was mechanically scribed at the border to remove shunts at the cut edges. After the first scribe (r_s = 10 mm) with high laser pulse energy and high overlap a substantial drop of the parallel resistance due to laser-induced shunt formation was found. Alterations of the laser power keeping constant the other parameters result in similar high shunt defect densities (section PS H1). Only when the pulse overlap is reduced (section PS L2) higher parallel resistances were achieved. Further, by varying different parameters for P3 scribing from Fig. 7 it is clearly seen that higher shunt resistances can be found for low pulse overlap. The highest parallel resistance in Fig. 7 was achieved at a pulse overlap of approximately 60%; the other parameters applied for this scribe are t_p = 10 ns; f = 10 kHz; E_p = 40 µJ; v_s = 100 mm/s.

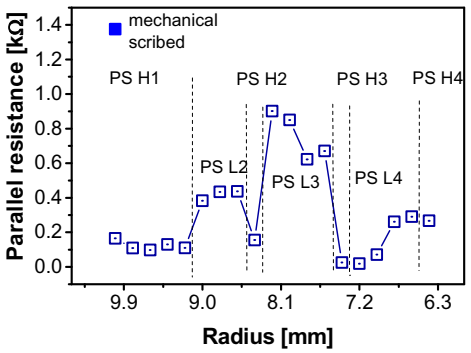

Fig. 7. Parallel resistance for CIGS solar cell material scribed with variable pulse length ns laser at selected parameter sets. L – low overlap of approx.. 30%. H – high overlap of approx. 60%; the highest parallel resistance achieved at these experiments is got at: r_s = 8.2 mm; t_p = 10 ns; f = 10 kHz; E_p = 20 µJ; v_s= 100 mm/s.

The measurement of the parallel resistance for ps laser scribing with the nested circular scribing approach shows that almost no significant shunts are formed with optimized laser scribing process parameters; the parallel resistance of mechanically scribed CIGS cells of approx. 1.2 kΩ can be preserved during ps laser scribing within a large laser fluence parameter field [17].

5. Conclusion

The in-process measurement technology provides an opportunity for a fast and reliable evaluation of the P3 laser scribing process for solar cells with respect to their electrical characteristics. Using this approach the parameters for P3 scribing with ns laser pulses were studied. A low pulse overlap has to be preferred in general for scribing with laser pulses of less than 10 ns. The reason for the achieved rather good electrical properties might be the short pulse rise time of this ns laser source that is independent on the pulse length. These particular laser pulse characteristics can establish different dynamic processes than those usually occur with other ns laser sources.

Acknowledgements

The authors acknowledge Mrs. Salamatin for the help in the manuscript preparation. This research has been partially supported by FP7 grant APPOLO No. 609355.

References

[1] T. Cheyney, Thin-film CIGS starts to come of age, Photovoltaics International, 1 (2008) 86-92.
[2] N. Gupta, Material selection for thin-film solar cells using multiple attribute decision making approach, Mater Design, 32 (2011) 1667-1671.
[3] EMPA announces 20.4% efficient thin film CIGS-on-polymer cell, in: pv magazine, http://www.pv-magazine.com/news/details/beitrag/empa-announces-204-efficient-thin-film-cigs-on-polymer-cell_100009893/#ixzz2OG4ZKLYB., 21, January 2013.
[4] G. Račiukaitis, P. Gečys, S. Grubinskas, K. Zimmer, M. Ehrhardt, A. Wehrmann, A. Braun, Laser structuring of thin films for flexible CIGS solar cells, Photovoltaics International, 17th Edition (2012) 91-98.
[5] G. Heise, M. Domke, J. Konrad, F. Pavic, M. Schmidt, H. Vogt, A. Heiss, J.r. Palm, H.P. Huber, Monolithical Serial Interconnects of Large CIS Solar Cells with Picosecond Laser Pulses, Physics Procedia, 12, Part B (2011) 149-155.
[6] A. Wehrmann, H. Schulte-Huxe, M. Ehrhardt, D. Ruthe, K. Zimmer, A. Braun, S. Ragnow, Change of electrical properties of CIGS thin-film solar cells after structuring with ultrashort laser pulses in: W. Pfleging, Y. Lu, K. Washio (Eds.) SPIE 7921 Laser-based Micro- and Nanopackaging and Assembly V, SPIE, San Fransisco, 2011, pp. 79210T-79214.
[7] A. Burn, V. Romano, M. Muralt, R. Witte, B. Frei, S. Bücheler, S. Nishiwaki, Selective ablation of thin films in latest generation CIGS solar cells with picosecond pulses, in, 2012, pp. 824318-824318-824317.
[8] N.G. Dhere, Scale-up issues of CIGS thin film PV modules, Sol. Energy Mater., 95 (2011) 277-280.
[9] A. Buzas, Z. Geretovszky, Nanosecond laser-induced selective removal of the active layer of CuInGaSe2 solar cells by stress-assisted ablation, Phys. Rev. B, 85 (2012).
[10] M. Rekow, D. Bartl, C. Sandfort, A. Letsch, Impact of P2 scribe geometry on monolithic series interconnected CIGS modules, in, 2013, pp. 86012J-86012J-86019.
[11] J. Bovatsek, A. Tamhankar, R.S. Patel, N.M. Bulgakova, J. Bonse, Thin film removal mechanisms in ns-laser processing of photovoltaic materials, Thin Solid Films, 518 (2010) 2897-2904.
[12] M. Ehrhardt, A. Wehrmann, P. Lorenz, K. Zimmer, Patterning of CIGS thin films induced by rear-side laser ablation of polyimide carrier foil, Applied Physics A, 113 (2013) 309-313.
[13] G. Raciukaitis, S. Grubinskas, P. Gecys, M. Gedvilas, Selectiveness of laser processing due to energy coupling localization: case of thin film solar cell scribing, Appl. Phys. A, 112 (2013) 93-98.
[14] S.H. Lee, C.K. Kim, J.H. In, H.S. Shim, S.H. Jeong, Selective removal of CuIn1-xGaxSe2 absorber layer with no edge melting using a nanosecond Nd : YAG laser, J. Phys. D, 46 (2013).
[15] P. Gečys, Ultrashort laser processing of thin-films for solar cells, in: Center for Physical Sciences and Technology, Institute of Physics, Vilnius University, Vilnius, 2012, pp. 139.
[16] X. Wang, M. Ehrhardt, P. Lorenz, C. Scheit, S. Ragnow, X.W. Ni, K. Zimmer, The influence of the laser parameter on the electrical shunt resistance of scribed Cu(InGa)Se2 solar cells by nested circular laser scribing technique, Appl. Surf. Sci., 302 (2014) 194-197.
[17] X. Wang, M. Ehrhardt, P. Lorenz, C. Scheit, S. Ragnow, X.W. Ni, K. Zimmer, In-process measuring of the electrical shunt resistance of laser-scribed thin-film stacks by nested circular scribes, Rev. Sci. Instrum., 84 (2013) 104704.
[18] G. Heise, M. Dickmann, M. Domke, A. Heiss, T. Kuznicki, J. Palm, I. Richter, H. Vogt, H.P. Huber, Investigation of the ablation of zinc oxide thin films on copper-indium-selenide layers by ps laser pulses, Appl. Phys. A, 104 (2011) 387-393.
[19] A.D. Compaan, I. Matulionis, S. Nakade, Laser scribing of polycrystalline thin films, Opt. Lasers Eng., 34 (2000) 15-45.